

FRACTAL HOMOGENIZATION OF MULTISCALE INTERFACE PROBLEMS

MARTIN HEIDA, RALF KORNHUBER, AND JOSCHA PODLESNY

ABSTRACT. Inspired by continuum mechanical contact problems with geological fault networks, we consider elliptic second order differential equations with jump conditions on a sequence of multiscale networks of interfaces with a finite number of non-separating scales. Our aim is to derive and analyze a description of the asymptotic limit of infinitely many scales in order to quantify the effect of resolving the network only up to some finite number of interfaces and to consider all further effects as homogeneous. As classical homogenization techniques are not suited for this kind of geometrical setting, we suggest a new concept, called fractal homogenization, to derive and analyze an asymptotic limit problem from a corresponding sequence of finite-scale interface problems. We provide an intuitive characterization of the corresponding fractal solution space in terms of generalized jumps and gradients together with continuous embeddings into L^2 and H^s , $s < 1/2$. We show existence and uniqueness of the solution of the asymptotic limit problem and exponential convergence of the approximating finite-scale solutions. Computational experiments involving a related numerical homogenization technique illustrate our theoretical findings.

This research has been funded by Deutsche Forschungsgemeinschaft (DFG) through grant CRC 1114 "Scaling Cascades in Complex Systems", Project C05 "Effective models for interfaces with many scales" and Project B01 "Fault networks and scaling properties of deformation accumulation".

1. INTRODUCTION

Classical elliptic homogenization is concerned with second order differential equations of the form

$$(1) \quad -\nabla(A^\varepsilon \nabla u_\varepsilon) = f,$$

denoting $A^\varepsilon(x) = A\left(\frac{x}{\varepsilon}\right)$ with $\varepsilon > 0$ and some uniformly bounded, positive coefficient field A . Hence, A^ε is oscillating on a spatial scale of size ε compared to the diameter of the macroscopic computational domain $Q \subset \mathbb{R}^d$. In periodic homogenization, the coefficient A is Y -periodic, where $Y = [0, 1]^d$ is the unit cell in \mathbb{R}^d . In stochastic homogenization, the coefficient $A^\varepsilon(x) = A_\omega\left(\frac{x}{\varepsilon}\right)$ is a stationary (i.e. statistically shift invariant) and ergodic (asymptotically uncorrelated) random variable on a probability space (Ω, \mathcal{F}, P) with $\omega \in \Omega$. A variety of results have been derived in the field of homogenization, and we refer to [1, 2, 11, 22] for the periodic case and to [24, 37] for the stochastic case. For error estimates in homogenization, we refer to [3, 4, 11, 17, 18]. Mathematical modelling of polycrystals or composite materials typically leads to elliptic interface problems with appropriate jump conditions on a microscopic interface $\Gamma^\varepsilon \subset Q$. A periodic setting is obtained by $\Gamma^\varepsilon = \varepsilon\Gamma_0$ with scaling parameter $\varepsilon > 0$ and a piecewise smooth hypermanifold Γ_0 with Y -periodic cells. The size of the cells is then of

order ε compared to the macroscopic domain. Denoting by $\llbracket u_\varepsilon \rrbracket_\nu$ the jump of u_ε in normal direction ν on Γ^ε , the condition

$$(2) \quad -\partial_\nu u_\varepsilon = \llbracket u_\varepsilon \rrbracket_\nu$$

on the normal derivatives $\partial_\nu u_\varepsilon$ is imposed at the boundary of each cell. Corresponding stochastic variants have been studied in [20, 23]. The homogenization of such kind of periodic multiscale interface problems has been studied in great detail, see [12, 13, 19, 21] and references therein. Similar concepts have been applied to foam-like elastic media like the human lung, cf., e.g., [5, 10]. Classical (stochastic) homogenization relies on periodicity (or ergodicity) and scale separation. The latter means that homogenized problems in the asymptotic limit $\varepsilon \rightarrow 0$ usually decouple into a global problem that describes the macroscopically observed behavior of the system, and one or more local problems, often referred to as *cell-problems*, that capture the oscillatory behavior.

In contrast to analytic homogenization, numerical homogenization addresses the lack of regularity of solutions of problems with highly oscillatory coefficients A^ε in numerical computations, either by local corrections of standard finite elements [14, 28] or by multigrid-type iterative schemes [26, 27]. Both approaches are closely related [25] and usually do not rely on periodicity or scale separation.

In this work, we consider elliptic multiscale interface problems without scale separation in a non-periodic geometric setting motivated by geology. Experimental studies suggest that grains in fractured rock are distributed in a fractal manner [30, 34]. In particular, this means that the size of grains and interfaces follows an exponential law: The total number $N(r)$ of grains larger than some $r > 0$ behaves according to

$$(3) \quad N(r) = Cr^{-D}$$

and D is often called the fractal dimension. This observation is also captured by geophysical modelling of fragmentation by tectonic deformation [33] which is based on the assumption that deformation of two neighboring blocks of equal size might lead to fracturing in one of these blocks. It is unlikely and therefore excluded in this model, that bigger blocks break smaller ones or vice versa. A typical example for corresponding multiscale interface networks is given by the Cantor-type geometry [34] as depicted in Figure 1. While each level- K interface network $\Gamma^{(K)}$ clearly is two-dimensional, the limiting multiscale network $\Gamma = \Gamma^{(\infty)}$ has fractal dimension $\ln 6 / \ln 2$, which is in good agreement with experimental studies that often yield $D \approx 2.5$. Observe that the cells representing the different grains are not periodically distributed. They can also be arbitrarily small and cover the whole range up to half of the given domain \mathbf{Q} so that there is no scale parameter ε separating a small from a large scale. Similar geometric settings, but with a completely different scope, occur for thin fractal fibers [29].

Geological applications give rise to continuum mechanical problems with frictional contact on such multiscale networks of interfaces or faults. The level- K network $\Gamma^{(K)} = \bigcup_{k=1}^K \Gamma_k$ consists of single faults Γ_k which are ordered from strong to weak in the sense that discontinuities of displacements along Γ_k are expected to decrease for increasing k , because “more fractured” media are expected to show higher resistance (for a more detailed discussion, see, e.g., [7, 16, 31] and the references cited therein).

In this paper, we restrict our considerations to scalar elliptic model problems on $\mathbf{Q} \setminus \Gamma^{(K)}$ for each level $K \in \mathbb{N}$ with weighted jumps along the network of interfaces $\Gamma^{(K)}$, instead of

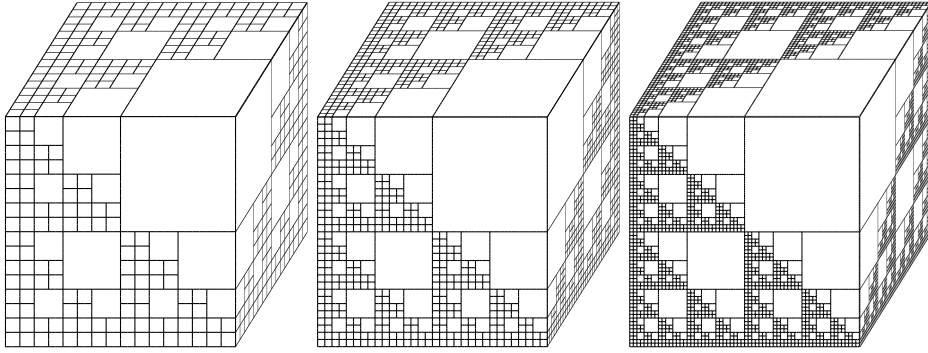


FIGURE 1. Level- K interface network $\Gamma^{(K)}$ for $K = 4, 5$, and 6 , taken from [34].

nonlinear frictional contact conditions. The ordering of the single interfaces Γ_k from strong to weak is reflected by scaling the contributions from the jumps along Γ_k in the corresponding energy functional with exponential weights $C_k(1 + \mathfrak{c})^k$. Here, $C_k > 0$ is a geometrical constant measuring the rate of fracturing for each k and $\mathfrak{c} > 0$ is a kind of material constant that determines the growth of resistance to jumps with increasing fracturing. We exploit the hierarchical structure of the interface networks $\Gamma^{(K)}$ to derive a hierarchy of solution spaces \mathcal{H}_K for the above-mentioned level- K interface problems. Under usual ellipticity conditions, the problems admit unique solutions $u_K \in \mathcal{H}_K$ for all $K \in \mathbb{N}$. The main concern of this paper is to investigate the asymptotic behavior of u_K for $K \rightarrow \infty$. As classical homogenization techniques are not suited for this purpose, we develop a new concept called *fractal homogenization*. The starting point is the construction of an asymptotic fractal limit space \mathcal{H} , that arises in a natural way by completion of the union of the level- K spaces \mathcal{H}_K , $K \in \mathbb{N}$. We provide continuous embeddings $\mathcal{H} \subset L^2$ and $\mathcal{H} \subset H^s$, $s < \frac{1}{2}$, and a characterization of \mathcal{H} in terms of generalized jumps and gradients. We then formulate a fractal limit problem associated with the level- K interface problems and show existence of a unique solution $u \in \mathcal{H}$ together with convergence $u_K \rightarrow u$ in \mathcal{H} . Imposing additional regularity assumptions on the geometry of the multiscale interface networks $\Gamma^{(K)}$, $K \in \mathbb{N}$, we are able to even show exponential estimates of the fractal homogenization error $\|u - u_K\|$ in \mathcal{H} for $K \rightarrow \infty$. In order to illustrate our theoretical findings by numerical experiments, we introduce a fractal numerical homogenization scheme in the spirit of [26, 27] that is based on a hierarchy of local patches from a hierarchy of meshes $\mathcal{T}_1, \dots, \mathcal{T}_K$ successively resolving the interfaces $\Gamma^{(1)}, \dots, \Gamma^{(K)}$. This decomposition induces an additive Schwarz preconditioner to accelerate the convergence of a conjugate gradient iteration. In numerical experiments with a Cantor-type geometry, we found the theoretically predicted behavior of (finite element approximations \tilde{u}_K of) u_K . We also observed that the convergence rates of our iterative scheme appear to be robust with respect to increasing K . Theoretical justification and extensions to model reduction in the spirit of [25, 28] are subject of current research.

The paper is structured as follows. In Section 2, we introduce multiscale interface networks together with associated level- K interface problems and prove existence and uniqueness of solutions u_K , $K \in \mathbb{N}$. In Section 3, we derive and analyze an associated fractal limit space \mathcal{H} and provide some basic properties, such as Sobolev embeddings and a Poincaré-type inequality. Then, we introduce a fractal interface problem, show existence of a unique solution $u \in \mathcal{H}$ as well as convergence $u_K \rightarrow u$ in \mathcal{H} . Exploiting additional assumptions on the geometry,

we prove exponential homogenization error estimates in Section 4. Section 5 is devoted to numerical computations based on (fractal) numerical homogenization techniques to illustrate our theoretical findings.

2. MULTISCALE INTERFACE PROBLEMS

2.1. Multiscale interface networks. Let $\mathbf{Q} \subset \mathbb{R}^d$ be a bounded domain with Lipschitz boundary $\partial\mathbf{Q}$ that contains mutually disjoint interfaces Γ_k , $k \in \mathbb{N}$. We assume that each interface Γ_k is piecewise affine and has finite $(d-1)$ -dimensional Hausdorff measure. We consider the multiscale interface network Γ and its level- K approximation $\Gamma^{(K)}$, given by

$$\Gamma = \bigcup_{k=1}^{\infty} \Gamma_k, \quad \Gamma^{(K)} = \bigcup_{k=1}^K \Gamma_k, \quad K \in \mathbb{N},$$

respectively. For each $K \in \mathbb{N}$, the set

$$\mathbf{Q} \setminus \Gamma^{(K)} = \bigcup_{G \in \mathcal{G}^{(K)}} G$$

splits into mutually disjoint, open, simply connected cells $G \in \mathcal{G}^{(K)}$ with the property $\partial G = \partial \overline{G}$. The subset of invariant cells is denoted by

$$\mathcal{G}_{\infty}^{(K)} = \left\{ G \in \mathcal{G}^{(K)} \mid G \in \mathcal{G}^{(L)} \ \forall L > K \right\},$$

and

$$(4) \quad d_K = \max \left\{ \text{diam } G \mid G \in \mathcal{G}^{(K)} \setminus \mathcal{G}_{\infty}^{(K)} \right\}$$

is the maximal size of cells $G \in \mathcal{G}^{(K)}$ to be divided on higher levels. Observe that $d_K \geq d_L$ holds for $L \geq K$. We assume

$$(5) \quad d_K \rightarrow 0 \quad \text{for} \quad K \rightarrow \infty.$$

Denoting

$$(x, y) = \{x + s(y - x) \mid s \in (0, 1)\},$$

and the number of elements of some set M by $\#M \in \mathbb{N} \cup \{+\infty\}$, we also assume that

$$(6) \quad \#(x, y) \cap \Gamma_k \leq C_k$$

holds for almost all $x, y \in \mathbf{Q}$ with $C_k \in \mathbb{N}$ depending only on $k \in \mathbb{N}$.

Example 2.1 (Cantor interface network in 3D [34]). *Consider the unit cube $\mathbb{I} = [0, 1]^3$ in \mathbb{R}^3 and the canonical basis $(e_i)_{i=1,2,3}$. Then $\Gamma^{(K)}$, $K \in \mathbb{N}$, is inductively constructed as follows. Set $\Gamma^{(0)} = \Gamma_0 = \partial\mathbb{I}$. For $k \in \mathbb{N} \cup \{0\}$ define*

$$\tilde{\Gamma}_{k+1} = \Gamma^{(k)} \cup \left(e_2 + \Gamma^{(k)} \right) \cup \left(e_3 + \Gamma^{(k)} \right) \cup \left(e_3 + e_1 + \Gamma^{(k)} \right) \cup \left(e_2 + e_1 + \Gamma^{(k)} \right) \cup \left(e_3 + e_2 + e_1 + \Gamma^{(k)} \right)$$

to obtain

$$\Gamma_{k+1} = \left(\frac{1}{2} \tilde{\Gamma}_{k+1} \right) \setminus \Gamma_k, \quad \Gamma^{(K+1)} = \Gamma^{(K)} \cup \Gamma_{k+1}.$$

Note that $\Gamma^{(K)}$ and $\Gamma = \bigcup_{k=1}^{\infty} \Gamma_k$ are self-similar by construction. We infer $d_K = 2^{-K}$ and $C_k = 2^{k-1}$.

See Figure 1 for an illustration of the Cantor interface networks $\Gamma^{(K)}$, $K = 4, 5, 6$. The construction process for a 2D-analogue is illustrated in Figure 2, where the newly added interfaces $\Gamma_1, \Gamma_2, \Gamma_3$, and Γ_4 are depicted in boldface in the four pictures from left to right.

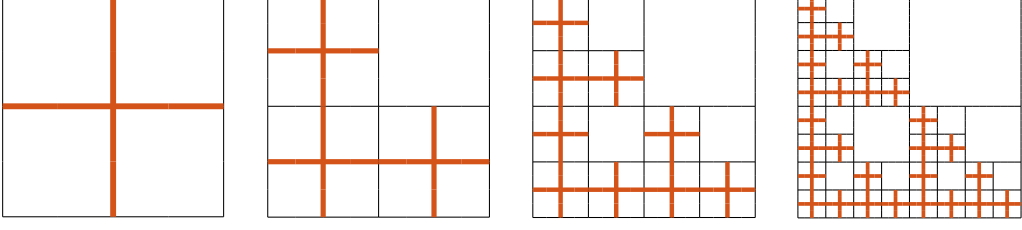


FIGURE 2. Construction of $\Gamma^{(K)}$, $K = 1, 2, 3, 4$ of a Cantor interface network in 2D.

Remark 2.2. Since all Γ_k , $k \in \mathbb{N}$, have Lebesgue measure zero in \mathbb{R}^d , their countable union Γ has Lebesgue measure zero as well. However, Γ might have fractal (Hausdorff-) dimension $d - s$ for some $s \in (0, 1)$ and infinite $(d - 1)$ -dimensional measure.

2.2. A multiscale hierarchy of Hilbert spaces. For each fixed $K \in \mathbb{N}$, we introduce the space

$$\mathcal{C}_{K,0}^1(\mathcal{Q}) = \left\{ v : \overline{\mathcal{Q}} \setminus \Gamma^{(K)} \rightarrow \mathbb{R} \mid v|_G \in C^1(\overline{G}) \ \forall G \in \mathcal{G}^{(K)} \text{ and } v|_{\partial \mathcal{Q}} \equiv 0 \right\}$$

of piecewise smooth functions on $\mathcal{Q} \setminus \Gamma^{(K)}$. Let $k = 1, \dots, K$. As Γ_k is piecewise affine, there is a normal ν_ξ to Γ_k at almost all $\xi \in \Gamma_k$ and we fix the orientation of ν_ξ such that $\nu_\xi \cdot e_m > 0$ with $m = \min\{i = 1, \dots, d \mid \nu_\xi \cdot e_i \neq 0\}$, and $\{e_1, \dots, e_d\}$ denotes the canonical basis of \mathbb{R}^d . For $\xi \in \Gamma^{(K)}$ such that ν_ξ exists and for $x \neq y \in \mathbb{R}^d$ such that $(x - y) \cdot \nu_\xi \neq 0$ the jump of $v \in \mathcal{C}_{K,0}^1(\mathcal{Q})$ across Γ_k at ξ in the direction $y - x$ is defined by

$$[[v]]_{x,y}(\xi) = \lim_{s \downarrow 0} (v(\xi + s(y - x)) - v(\xi - s(y - x))) .$$

Up to the sign, $[[v]]_{x,y}(\xi)$ is equal to the normal jump of $v \in \mathcal{C}_{K,0}^1(\mathcal{Q})$

$$[[v]](\xi) := [[v]]_{\xi - \nu_\xi, \xi + \nu_\xi}(\xi)$$

and defined at almost all $\xi \in \Gamma_k$.

For some fixed material constant $\mathfrak{c} > 0$, that determines the growth of resistance to jumps with increasing fracturing, and the geometrical constant C_k taken from (6), we introduce the scalar product

$$(7) \quad \langle v, w \rangle_{K,\mathfrak{c}} = \int_{\mathcal{Q} \setminus \Gamma^{(K)}} \nabla v \cdot \nabla w \, dx + \sum_{k=1}^K (1 + \mathfrak{c})^k C_k \int_{\Gamma_k} [[v]] [[w]] \, d\Gamma_k, \quad v, w \in \mathcal{C}_{K,0}^1(\mathcal{Q}),$$

with the associated norm $\|v\|_{K,\mathfrak{c}} = \langle v, v \rangle_{K,\mathfrak{c}}^{1/2}$. Observe that $(1 + \mathfrak{c})^k$ generates an exponential scaling of the resistance to jumps across Γ_k .

We set

$$(8) \quad \mathcal{H}_K = \text{closure}_{\|\cdot\|_{K,\mathfrak{c}}} \mathcal{C}_{K,0}^1(\mathcal{Q})$$

to finally obtain a hierarchy of Hilbert spaces

$$(9) \quad \mathcal{H}_1 \subset \dots \subset \mathcal{H}_{K-1} \subset \mathcal{H}_K, \quad K \in \mathbb{N},$$

with isometric embeddings.

2.3. Level- K interface problems. For a given measurable function

$$(10) \quad A : \Gamma \rightarrow \mathbb{R}$$

satisfying

$$(11) \quad 0 < \mathfrak{a} \leq A(x) \leq \mathfrak{A} < \infty \quad \text{a.e. on } \Gamma$$

with suitable $\mathfrak{a}, \mathfrak{A} \in \mathbb{R}$ and each $K \in \mathbb{N}$, we define the symmetric bilinear form

$$a_K(v, w) = \int_{Q \setminus \Gamma^{(K)}} \nabla v \cdot \nabla w \, dx + \sum_{k=1}^K (1 + \mathfrak{c})^k C_k \int_{\Gamma_k} A[v][w] \, d\Gamma_k \quad v, w \in \mathcal{H}_K.$$

For ease of presentation, we assume $\mathfrak{a} \leq 1 \leq \mathfrak{A}$ without loss of generality. Then $a_K(\cdot, \cdot)$ is uniformly coercive and bounded on \mathcal{H}_K in the sense that

$$\mathfrak{a} \|v\|_{K, \mathfrak{c}}^2 \leq a_K(v, v), \quad a_K(v, w) \leq \mathfrak{A} \|v\|_{K, \mathfrak{c}} \|w\|_{K, \mathfrak{c}}$$

holds for all $K \in \mathbb{N}$. With given functional $\ell \in \mathcal{H}'_K$, $K \in \mathbb{N}$, from the associated dual space, we consider the following minimization problem.

Problem 2.3 (Level- K interface problem). *For fixed $K \in \mathbb{N}$, find a minimizer $u_K \in \mathcal{H}_K$ of the energy functional*

$$(12) \quad \mathcal{E}_K(v) = \frac{1}{2} a_K(v, v) - \ell(v), \quad v \in \mathcal{H}_K.$$

The following proposition is an immediate consequence of the Lax-Milgram lemma.

Proposition 2.4. *Problem 2.3 is equivalent to the variational problem of finding $u_K \in \mathcal{H}_K$ such that*

$$(13) \quad a_K(u_K, v) = \ell(v) \quad \forall v \in \mathcal{H}_K$$

and admits a unique solution.

Successive resolution of the multiscale interface network Γ by level- K approximations $\Gamma^{(K)}$ with increasing $K \in \mathbb{N}$ motivates investigation of the asymptotic behavior of finite level solutions u_K for $K \rightarrow \infty$. This will be the subject of the next section.

3. FRACTAL HOMOGENIZATION

3.1. Fractal function spaces. We consider the pre-Hilbert space

$$\mathcal{H}^\circ = \bigcup_{K=1}^{\infty} \mathcal{H}_K$$

equipped with the scalar product defined by

$$\langle v, w \rangle_{\mathfrak{c}} = \langle v, w \rangle_{\max\{K, L\}, \mathfrak{c}}, \quad v \in \mathcal{H}_L, \, w \in \mathcal{H}_K,$$

and associated norm $\|\cdot\|_{\mathfrak{c}} = \langle \cdot, \cdot \rangle_{\mathfrak{c}}^{1/2}$. A Hilbert space with dense subspace \mathcal{H}° is obtained by classical completion.

Definition 3.1 (Fractal space). *The fractal space $\mathcal{H}_{\mathfrak{c}}$ consists of all equivalence classes of Cauchy sequences $(v_K)_{K \in \mathbb{N}}$ in \mathcal{H}° with respect to the equivalence relation*

$$(v_K)_{K \in \mathbb{N}} \sim (w_K)_{K \in \mathbb{N}} \iff \|v_K - w_K\|_{\mathfrak{c}} \rightarrow 0 \text{ for } K \rightarrow \infty.$$

For each Cauchy sequence in \mathcal{H}° , we can find an equivalent Cauchy sequence $(v_K)_{K \in \mathbb{N}}$ in \mathcal{H}° such that $v_K \in \mathcal{H}_K$, $K \in \mathbb{N}$, by exploiting the hierarchy (9). We always use such a representative of elements of $\mathcal{H}_\mathfrak{c}$. The following result is a well-known consequence of the construction of $\mathcal{H}_\mathfrak{c}$.

Proposition 3.2. *The fractal space $\mathcal{H}_\mathfrak{c}$ is a Hilbert space equipped with the scalar product*

$$(14) \quad \langle v, w \rangle_\mathfrak{c} = \lim_{K \rightarrow \infty} \langle v_K, w_K \rangle_{K, \mathfrak{c}}, \quad v = (v_K)_{K \in \mathbb{N}}, \quad w = (w_K)_{K \in \mathbb{N}} \in \mathcal{H}_\mathfrak{c}$$

and associated norm $\|\cdot\|_\mathfrak{c} = \langle \cdot, \cdot \rangle_\mathfrak{c}^{1/2}$.

From now on, we identify the spaces \mathcal{H}_K with their isometric embeddings in $\mathcal{H}_\mathfrak{c}$ defined by

$$\mathcal{H}_K \ni v_K \mapsto (v_L)_{L \in \mathbb{N}} \in \mathcal{H}_\mathfrak{c} \quad \text{with } v_L = v_K, \text{ if } L \geq K \text{ and } v_L = 0 \text{ else.}$$

By construction, we have the following approximation result.

Proposition 3.3. *For any fixed $\mathfrak{c} > 0$, the hierarchy*

$$(15) \quad \mathcal{H}_1 \subset \cdots \subset \mathcal{H}_K \subset \cdots \subset \mathcal{H}_\mathfrak{c}$$

consists of closed subspaces \mathcal{H}_K of $\mathcal{H}_\mathfrak{c}$, $K \in \mathbb{N}$, with the property

$$(16) \quad \inf_{v \in \mathcal{H}_K} \|w - v\|_\mathfrak{c} \rightarrow 0 \quad \text{for } K \rightarrow \infty \quad \forall w \in \mathcal{H}_\mathfrak{c},$$

and $\cup_{K \in \mathbb{N}} \mathcal{C}_{K,0}^1(\mathcal{Q})$ is dense in $\mathcal{H}_\mathfrak{c}$.

Remark 3.4. *For each fixed $K \in \mathbb{N}$, the spaces \mathcal{H}_K are independent of \mathfrak{c} . This is no longer the case for the limit space $\mathcal{H}_\mathfrak{c}$, because $v = (v_K)_{K \in \mathbb{N}} \in \mathcal{H}_\mathfrak{c}$ for a certain $\mathfrak{c} > 0$ implies that the jumps $\|v_K\|_{L^2(\Gamma_k)}$ are decreasing fast enough to compensate the exponential weights $C_k(1 + \mathfrak{c})^k$ for this \mathfrak{c} , which might no longer be the case for larger weights $C_k(1 + \mathfrak{c}')^k$ with some $\mathfrak{c}' > \mathfrak{c}$ so that $v \notin \mathcal{H}_{\mathfrak{c}'}$.*

From now on, we will mostly skip the subscript \mathfrak{c} for notational convenience. A more intuitive representation of the scalar product $\langle \cdot, \cdot \rangle$ in \mathcal{H} and its associated norm $\|\cdot\|$ in terms of generalized jumps and gradients will be derived in Section 3.3 below.

3.2. Sobolev embeddings. We now investigate the embedding of the fractal space \mathcal{H} into the fractional Sobolev spaces $H^s(\mathcal{Q})$, $s \in (0, \frac{1}{2})$, equipped with the Sobolev-Slobodeckij norm

$$\|v\|_{H^s(\mathcal{Q})} = \left(\int_{\mathcal{Q}} |v|^2 dx + \int_{\mathcal{Q}} \int_{\mathcal{Q}} \frac{|v(x) - v(y)|^2}{|x - y|^{d+2s}} dx dy \right)^{\frac{1}{2}}.$$

Lemma 3.5. *Let $K \in \mathbb{N}$, $v \in \mathcal{C}_{K,0}^1(\mathcal{Q})$, and $x \neq y \in \mathcal{Q}$. Then the following inequality holds for every $\mathfrak{c} > 0$ and for a.e. $x, y \in \mathbb{R}^d$*

$$(17) \quad \begin{aligned} |v(x) - v(y)|^2 &\leq \left(1 + \frac{1}{\mathfrak{c}}\right) |x - y|^2 \int_0^1 |\nabla v(x + s(y - x))|^2 ds \\ &\quad + \left(1 + \frac{1}{\mathfrak{c}}\right) \sum_{k=1}^K (1 + \mathfrak{c})^k C_k \sum_{\xi \in (x,y) \cap \Gamma_k} \|v\|_{x,y}^2(\xi), \end{aligned}$$

where $\nabla v(x + s(y - x))$ is understood to be zero, if $x + s(y - x) \in \Gamma^{(K)}$.

Proof. Let x, y be such that $(x, y) \cap \Gamma^{(K)}$ is finite. Using the Cauchy-Schwarz inequality and the binomial estimate $2ab < \frac{1}{c}a^2 + cb^2$ with $c > 0$ and $a, b \in \mathbb{R}$, we infer

$$\begin{aligned} |v(x) - v(y)|^2 &\leq \left(\sum_{k=1}^K \sum_{\xi \in (x,y) \cap \Gamma_k} \llbracket v \rrbracket_{x,y}(\xi) + \int_0^1 \nabla v(x + s(y-x)) \cdot (y-x) \, ds \right)^2 \\ &\leq \left(1 + \frac{1}{c}\right) |x-y|^2 \int_0^1 |\nabla v(x + s(y-x))|^2 \, ds + (1+c) \left(\sum_{k=1}^K \sum_{\xi \in (x,y) \cap \Gamma_k} \llbracket v \rrbracket_{x,y}(\xi) \right)^2 \\ &\leq \left(1 + \frac{1}{c}\right) |x-y|^2 \int_0^1 |\nabla v(x + s(y-x))|^2 \, ds \\ &\quad + (1+c) \left(1 + \frac{1}{c}\right) \left(\sum_{\xi \in (x,y) \cap \Gamma_1} \llbracket v \rrbracket_{x,y}(\xi) \right)^2 + (1+c)^2 \left(\sum_{k=2}^K \sum_{\xi \in (x,y) \cap \Gamma_k} \llbracket v \rrbracket_{x,y}(\xi) \right)^2. \end{aligned}$$

According to the Cauchy-Schwarz inequality and the definition of C_k in (6), we have

$$\left(\sum_{\xi \in (x,y) \cap \Gamma_k} \llbracket v \rrbracket_{x,y}(\xi) \right)^2 \leq C_k \sum_{\xi \in (x,y) \cap \Gamma_k} \llbracket v \rrbracket_{x,y}^2(\xi)$$

and the assertion follows by induction. \square

We are ready to state the main result of this subsection.

Theorem 3.6. *The continuous embeddings*

$$(18) \quad \mathcal{H}_c \subset L^2(\mathbf{Q}) \quad \text{and} \quad \mathcal{H}_c \subset H^s(\mathbf{Q})$$

hold for every $c > 0$ and every $s \in [0, \frac{1}{2})$. In particular, the following Poincaré-type inequality

$$(19) \quad \|v\|_{L^2(\mathbf{Q})}^2 \leq C_0 \left(\|\nabla v\|_{L^2(\mathbf{Q} \setminus \Gamma)}^2 + \sum_{k=1}^{\infty} (1+c)^k C_k \|\llbracket v \rrbracket\|_{L^2(\Gamma_k)}^2 \right),$$

holds with $C_0 = (1 + \frac{1}{c}) \text{diam}(\mathbf{Q}) \max\{\text{diam}(\mathbf{Q}), 1\}$.

Proof. We use an approach introduced by Hummel [23]. Let $K \in \mathbb{N}$, $v \in \mathcal{C}_{K,0}^1(\mathbf{Q})$, and $k = 1, \dots, K$. We extend v by zero to a function $v : \mathbb{R}^d \rightarrow \mathbb{R}$, fix some $\eta > 0$ to be specified later, and consider the orthonormal basis $(e_i)_{i=1,\dots,d}$ of \mathbb{R}^d . Exploiting that the determinant g_k of the first fundamental form of Γ_k satisfies $g_k \geq 1$, we obtain

$$\begin{aligned} \int_{\mathbf{Q}} \sum_{\xi \in (x, x+\eta e_1) \cap \Gamma_k} \llbracket v \rrbracket_{x, x+\eta e_1}^2(\xi) \, dx &\leq \int_{\mathbb{R}} \left(\int_{\mathbb{R}^{d-1}} \sum_{\xi \in (x, x+\eta e_1) \cap \Gamma_k} \llbracket v \rrbracket_{x, x+\eta e_1}^2(\xi) \sqrt{g_k} \, dx_2 \dots dx_d \right) dx_1 \\ &\leq \int_{\mathbb{R}} \left(\int_{\Gamma_k \cap ((x_1, x_1+\eta) \times \mathbb{R}^{d-1})} \llbracket v \rrbracket_{x, x+\eta e_1}^2(\xi) \, d\Gamma_k \right) dx_1 \\ &= \int_{\Gamma_k} \left(\int_{\xi_1-\eta}^{\xi_1} \llbracket v \rrbracket_{x, x+\eta e_1}^2 \, dx_1 \right) (\xi) \, d\Gamma_k = \eta \int_{\Gamma_k} \llbracket v \rrbracket^2(\xi) \, d\Gamma_k, \end{aligned}$$

where we used that $\llbracket v \rrbracket^2(\xi)$ is well defined a.e. on Γ_k and $\xi = (\xi_1, \xi') \in \Gamma_k \cap ((x_1, x_1 + \eta) \times \mathbb{R}^{d-1})$ is equivalent to $x_1 \in (\xi_1 - \eta, \xi_1)$ with $\xi = (\xi_1, \xi') \in \Gamma_k$. The same arguments provide

$$(20) \quad \int_{\mathbf{Q}} \sum_{\xi \in (x, x+\eta e) \cap \Gamma_k} \llbracket v \rrbracket^2(\xi) dx \leq \eta \int_{\Gamma_k} \llbracket v \rrbracket^2 d\Gamma_k$$

for any unit vector $e \in \mathbb{R}^d$. Inserting (20) after integrating (17) with $y = x + \eta e$ over \mathbf{Q} leads to

$$(21) \quad \int_{\mathbf{Q}} |v(x) - v(x + \eta e)|^2 dx \leq \eta \left(1 + \frac{1}{\mathfrak{c}}\right) \left(\eta \|\nabla v\|_{L^2(\mathbf{Q} \setminus \Gamma^{(K)})}^2 + \sum_{k=1}^K (1 + \mathfrak{c})^k C_k \|\llbracket v \rrbracket\|_{L^2(\Gamma_k)}^2 \right).$$

We select $\eta \geq \text{diam}(\mathbf{Q})$ to obtain the Poincaré-type inequality (19) and thus $\mathcal{H}_{\mathfrak{c}} \subset L^2(\mathbf{Q})$.

Next, we divide (21) by $|\eta|^{d+2s}$ and integrate over

$$\mathbf{Q} \subset \{\eta e \mid \eta \leq \text{diam}(\mathbf{Q}), e \in \mathbb{S}^d\},$$

where \mathbb{S}^d denotes the unit sphere in \mathbb{R}^d , to find that

$$(22) \quad \|v\|_{H^s(\mathbf{Q})}^2 \leq \left(1 + \frac{1}{\mathfrak{c}}\right) C_s \left(\|\nabla v\|_{L^2(\mathbf{Q} \setminus \Gamma^{(K)})}^2 + \sum_{k=1}^K (1 + \mathfrak{c})^k C_k \|\llbracket v \rrbracket\|_{L^2(\Gamma_k)}^2 \right)$$

holds for all $v \in \mathcal{C}_{K,0}^1(\mathbf{Q})$ and all $K \in \mathbb{N}$ with $C_s = \max\{\text{diam}(\mathbf{Q}), 1\} |\mathbb{S}^d| \int_0^{\text{diam}(\mathbf{Q})} \eta^{-2s} d\eta < \infty$ for every $s \in [0, \frac{1}{2})$. By Proposition 3.3, the subspace $\cup_{K \in \mathbb{N}} \mathcal{C}_{K,0}^1(\mathbf{Q})$ is dense in \mathcal{H} . This concludes the proof. \square

Remark 3.7. For any given $(v_K)_{K \in \mathbb{N}} \in \mathcal{H}$, there is a unique $v \in \cap_{0 < s < \frac{1}{2}} H^s(\mathbf{Q})$ such that

$$(23) \quad \|v - v_K\|_{H^s(\mathbf{Q})} \rightarrow 0 \quad \text{for } K \rightarrow \infty \quad \forall s \in (0, \frac{1}{2})$$

as a consequence of Theorem 3.6.

3.3. Weak gradients and generalized jumps. Let $(v_K)_{K \in \mathbb{N}} \in \mathcal{H}$ and observe that

$$\mathbf{Q} \setminus \Gamma = \mathbf{Q} \cap \left(\bigcup_{k=1}^{\infty} \Gamma_k \right)^c \subset \mathbf{Q} \setminus \Gamma^{(K)}$$

is Lebesgue measurable. Hence, we have

$$\|\nabla v_K\|_{L^2(\mathbf{Q} \setminus \Gamma)}^2 + \sum_{k=1}^K (1 + \mathfrak{c})^k C_k \|\llbracket v_K \rrbracket\|_{L^2(\Gamma_k)}^2 \leq \|v_K\|_K^2 \quad \forall K \in \mathbb{N}.$$

Therefore, $(\nabla v_K)_{K \in \mathbb{N}}$ and $(\llbracket v_K \rrbracket)_{K \in \mathbb{N}}$ are Cauchy sequences in $L^2(\mathbf{Q} \setminus \Gamma)^d$ and in the sequence space $(L^2(\Gamma_k))_{k \in \mathbb{N}}$ equipped with the weighted norm

$$\|j\|_{\Gamma} = \left(\sum_{k=1}^{\infty} (1 + \mathfrak{c})^k C_k \|j_k\|_{L^2(\Gamma_k)}^2 \right)^{\frac{1}{2}}, \quad j = (j_k)_{k \in \mathbb{N}} \in (L^2(\Gamma_k))_{k \in \mathbb{N}},$$

respectively. In light of the completeness of $L^2(\mathbf{Q} \setminus \Gamma)^d$ and of $(L^2(\Gamma_k))_{k \in \mathbb{N}}$, this leads to the following definition.

Definition 3.8. Let $(v_K)_{K \in \mathbb{N}} \in \mathcal{H}$ with associated $v \in \cap_{0 < s < \frac{1}{2}} H^s(\mathbf{Q})$ that is characterized by (23). Then the limits

$$\nabla v = \lim_{K \rightarrow \infty} \nabla v_K \quad \text{in } L^2(\mathbf{Q} \setminus \Gamma) \quad \text{and} \quad \llbracket v \rrbracket = \lim_{K \rightarrow \infty} \llbracket v_K \rrbracket \quad \text{in } (L^2(\Gamma_k))_{k \in \mathbb{N}}$$

are called the weak gradient and generalized jump of v , respectively.

Since the fractal (and Hausdorff-) dimension of Γ might be larger than $d-1$, it is not obvious to define $L^2(\Gamma)$ (and to infer convergence of $(\llbracket u_K \rrbracket)_{K \in \mathbb{N}}$ in $L^2(\Gamma)$), because it is not obvious which measure to choose.

Proposition 3.9. *Let $(v_K)_{K \in \mathbb{N}} \in \mathcal{H}$ with associated $v \in \cap_{0 < s < \frac{1}{2}} H^s(\mathbf{Q})$ that is characterized by (23). Then the weak gradient ∇v and the generalized jump $\llbracket v \rrbracket$ of v are related by the identity*

$$(24) \quad \int_{\mathbf{Q}} v \nabla \cdot \varphi \, dx = - \int_{\mathbf{Q} \setminus \Gamma} \nabla v \cdot \varphi \, dx + \sum_{k=1}^{\infty} \int_{\Gamma_k} \llbracket v \rrbracket \varphi \cdot \nu_k \, d\Gamma_k \quad \forall \varphi \in C_0^\infty(\mathbb{R}^d)^d.$$

Proof. Let $\varphi \in C_0^\infty(\mathbb{R}^d)^d$ and recall that Γ has Lebesgue measure zero in \mathbb{R}^d according to Remark 2.2. As a consequence, we have

$$\int_{\mathbf{Q} \setminus \Gamma^{(K)}} \nabla v_K \cdot \varphi \, dx = \int_{\mathbf{Q} \setminus \Gamma} \nabla v_K \cdot \varphi \, dx + \int_{\Gamma \setminus \Gamma^{(K)}} \nabla v_K \cdot \varphi \, dx \rightarrow \int_{\mathbf{Q} \setminus \Gamma} \nabla v \cdot \varphi \, dx \quad \text{for } K \rightarrow \infty$$

which by Definition 3.8 leads to

$$\begin{aligned} \int_{\mathbf{Q}} v \nabla \cdot \varphi \, dx &= \lim_{K \rightarrow \infty} \int_{\mathbf{Q}} v_K \nabla \cdot \varphi \, dx \\ &= \lim_{K \rightarrow \infty} \left(- \int_{\mathbf{Q} \setminus \Gamma^{(K)}} \nabla v_K \cdot \varphi \, dx + \sum_{k=1}^K \int_{\Gamma_k} \llbracket v_K \rrbracket \varphi \cdot \nu_k \, d\Gamma_k \right) \\ &= - \int_{\mathbf{Q} \setminus \Gamma} \nabla v \cdot \varphi \, dx + \sum_{k=1}^{\infty} \int_{\Gamma_k} \llbracket v \rrbracket \varphi \cdot \nu_k \, d\Gamma_k. \end{aligned}$$

□

Theorem 3.10. *Let $v_{\mathcal{H}} = (v_K)_{K \in \mathbb{N}}, w_{\mathcal{H}} = (w_K)_{K \in \mathbb{N}} \in \mathcal{H}$ with associated $v, w \in \cap_{0 < s < \frac{1}{2}} H^s(\mathbf{Q})$ that are characterized by (23). Then we have*

$$(25) \quad \langle v_{\mathcal{H}}, w_{\mathcal{H}} \rangle = \int_{\mathbf{Q} \setminus \Gamma} \nabla v \cdot \nabla w \, dx + \sum_{k=1}^{\infty} (1 + \mathfrak{c})^k C_k \int_{\Gamma_k} \llbracket v \rrbracket \llbracket w \rrbracket \, d\Gamma_k.$$

Proof. By Definition 3.8 of generalized jumps, we have

$$\sum_{k=1}^K (1 + \mathfrak{c})^k C_k \int_{\Gamma_k} \llbracket v_K \rrbracket \llbracket w_K \rrbracket \, d\Gamma_k \rightarrow \sum_{k=1}^{\infty} (1 + \mathfrak{c})^k C_k \int_{\Gamma_k} \llbracket v \rrbracket \llbracket w \rrbracket \, d\Gamma_k \quad \text{for } K \rightarrow \infty$$

and as Γ has Lebesgue measure zero in \mathbb{R}^d (cf. Remark 2.2), we obtain

$$\int_{\mathbf{Q} \setminus \Gamma^{(K)}} \nabla v_K \cdot \nabla w_K \, dx = \int_{\mathbf{Q} \setminus \Gamma} \nabla v_K \cdot \nabla w_K \, dx \rightarrow \int_{\mathbf{Q} \setminus \Gamma} \nabla v \cdot \nabla w \, dx \quad \text{for } K \rightarrow \infty.$$

This concludes the proof. □

From now on, we identify $(v_K)_{K \in \mathbb{N}} \in \mathcal{H}$ with $v \in \cap_{0 < s < \frac{1}{2}} H^s(\mathbf{Q})$ characterized by (23) and use the representation (25) of the scalar product $\langle \cdot, \cdot \rangle$ in \mathcal{H} .

For the Cantor interface network, cf. Example 2.1, the weighting factors $(1 + \mathfrak{c})^k C_k$ in (25) are exponentially increasing with k , causing exponentially decreasing generalized jumps across Γ_k .

3.4. Fractal interface problems. We consider the functional

$$\ell(v) = \int_Q f v \, dx$$

with some given $f \in L^2(Q)$. Note that the Poincaré-type inequality (19) implies $\ell \in \mathcal{H}' \subset \mathcal{H}'_K$ for all $K \in \mathbb{N}$. The solutions u_K of the level- K interface Problems 2.3 for $K \in \mathbb{N}$ then satisfy the uniform stability estimate

$$(26) \quad \|u_K\| \leq C_0 \mathfrak{a}^{-1} \|f\|_{L^2(Q)}, \quad K \in \mathbb{N},$$

with the constant C_0 appearing in (19).

We define the symmetric bilinear form

$$(27) \quad a(v, w) = \int_{Q \setminus \Gamma} \nabla v \cdot \nabla w \, dx + \sum_{k=1}^{\infty} (1 + \mathfrak{c})^k C_k \int_{\Gamma_k} A \llbracket v \rrbracket \llbracket w \rrbracket \, d\Gamma_k, \quad v, w \in \mathcal{H},$$

with $A : \Gamma \rightarrow \mathbb{R}$ taken from (10). Note that $a(\cdot, \cdot)$ is well-defined, coercive and bounded in light of Definition 3.8 and assumption (11). Now, we are ready to formulate an asymptotic limit of the level- K interface Problems 2.3 for $K \rightarrow \infty$.

Problem 3.11 (Fractal interface problem). *Find a minimizer $u \in \mathcal{H}$ of the energy functional*

$$\mathcal{E}(v) = \frac{1}{2} a(v, v) - \ell(v), \quad v \in \mathcal{H}.$$

In light of Proposition 3.3, the following existence and approximation result is a consequence of the Lax-Milgram lemma and Céa's lemma.

Theorem 3.12. *Problem 3.11 is equivalent to the variational problem of finding $u \in \mathcal{H}$ such that*

$$(28) \quad a(u, v) = \ell(v) \quad \forall v \in \mathcal{H}$$

and admits a unique solution. Moreover, the error estimate

$$(29) \quad \|u - u_K\| \leq \frac{\mathfrak{A}}{\mathfrak{a}} \inf_{v \in \mathcal{H}_K} \|u - v\|$$

implies convergence $\|u - u_K\| \rightarrow 0$ for $K \rightarrow \infty$.

In the next section, we will improve the straightforward error estimate (29) under more restrictive assumptions on the geometry of the multiscale interface network.

4. EXPONENTIAL ERROR ESTIMATES

We concentrate on the special case that all cells $G \in \mathcal{G}^{(K)}$, $K \in \mathbb{N}$, are hyper-cuboids with edges $e_{G,i}$, $i = 1, \dots, d2^{d-1}$, either parallel or perpendicular to the unit vectors e_i , $i = 1, \dots, d$. For $K \in \mathbb{N}$, we set

$$d_G^{\max} = \max_i |e_{G,i}|, \quad d_G^{\min} = \min_i |e_{G,i}|, \quad G \in \mathcal{G}^{(K)}, \quad \text{and} \quad d_K^{\min} = \min_{G \in \mathcal{G}^{(K)}} d_G^{\min},$$

and assume that there is a constant $\mathfrak{g} > 0$ such that

$$(30) \quad d^{-1/2} d_K \leq d_G^{\max} \leq d^{-1/2} \mathfrak{g} d_G^{\min} \quad \forall G \in \mathcal{G}^{(K)}, \quad K \in \mathbb{N},$$

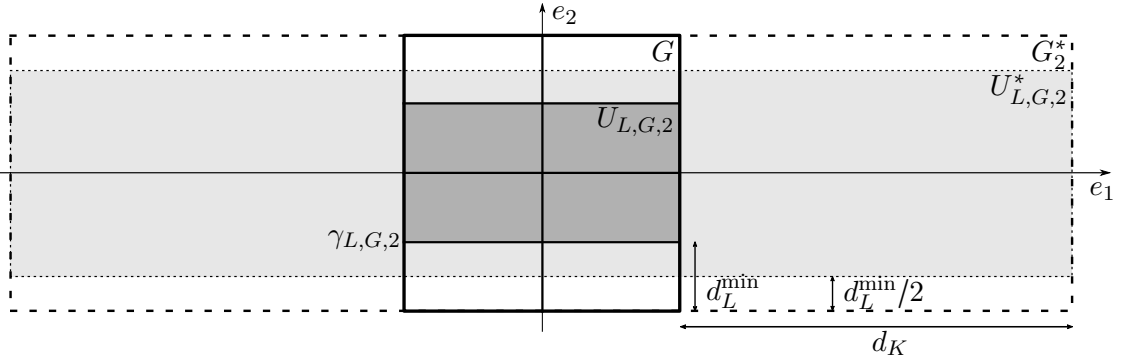


FIGURE 3. Construction of $\xi_{L,G,i}$: $G \in \mathcal{G}^{(K)} \setminus \mathcal{G}_\infty^{(K)}$ with $\Gamma^{(L)} \cap G = \gamma_{L,G,1} \cup \gamma_{L,G,2}$ and G_2^* (dashed), light-grey $U_{L,G,2}^*$, and dark-grey $U_{L,G,2}$.

with space dimension d and d_K taken from (4). Note that (30) implies uniform shape regularity of all $G \in \mathcal{G}^{(K)}$ together with quasi-uniformity of the partition $\mathcal{G}^{(K)} \setminus \mathcal{G}_\infty^{(K)}$. We also assume that $\mathcal{G}^{(K)}$ is regular for all $K \in \mathbb{N}$ in the sense that two cells $G \in \mathcal{G}^{(K)} \setminus \mathcal{G}_\infty^{(K)}$ and $G' \in \mathcal{G}^{(K)}$ have an intersection $F = G \cap G'$ with non-zero $(d-1)$ -dimensional Hausdorff measure, if and only if F is a common $(d-1)$ -face of G and G' . Note that the Cantor set described in subsection 2.1 satisfies both of these additional assumptions.

The derivation of error estimates will rely on a representation of the residual of the approximate solution u_K of Problem 2.3 in terms of its normal traces on Γ_L , $L > K$ (cf., e.g., variational formulations of substructuring methods [32]). This requires additional regularity in a neighborhood of Γ_L , $L > K$.

Lemma 4.1. *Let $K \in \mathbb{N}$, $G \in \mathcal{G}^{(K)} \setminus \mathcal{G}_\infty^{(K)}$, $L > K$, and $\Gamma_L \cap G = \bigcup_{i=1}^d \gamma_{L,G,i}$, such that $e_i \perp \gamma_{L,G,i}$, $i = 1, \dots, d$. Then, for each $i = 1, \dots, d$ there are open sets $U_{L,G,i} \subset G$ with $\gamma_{L,G,i} \subset U_{L,G,i}$ such that $\partial_i u_K \in H^1(U_{L,G,i})$ and the a priori estimate*

$$(31) \quad d_L \|\partial_i u_K\|_{L^2(\gamma_{L,G,i})}^2 \leq c \left(d_L^2 \|f\|_{L^2(G_i^*)}^2 + \|\partial_i u_K\|_{L^2(G_i^* \setminus \Gamma^{(K)})}^2 \right)$$

holds with a constant c depending only on \mathfrak{g} and d .

Proof. The main idea of the proof is to first provide local a priori H^1 -bounds for difference quotients $D_i^h u_K = \frac{1}{h} (u_K(\cdot + e_i h) - u_K)$ that are uniform in h on suitable subsets $U_{L,G,i}$. These H^1 -bounds then lead to related H^1 -bounds for $\partial_i u_K$ by well-known arguments from Evans [15] so that the desired a priori estimates (31) finally follow from the trace theorem. Most part the proof is devoted to the local a priori H^1 -bounds for $D_i^h u_K$. They are derived from the weak formulation (2.3) of the problem by inserting test functions of the form $v = -D_i^{-h} (\xi^2 D_i^h) u_K \in \mathcal{H}_K$ with sophisticatedly constructed smooth functions $\xi = \xi_{L,G,i}$ with local support in some suitable $U_{L,G,i}^*$ and $\xi \equiv 1$ on the final subset $U_{L,G,i} \subset U_{L,G,i}^*$.

Let $G = (-g, g)^d \in \mathcal{G}^{(K)} \setminus \mathcal{G}_\infty^{(K)}$, for simplicity, and consider some fixed $i = 1, \dots, d$. We start with the construction of $\xi_{L,G,i}$ which is illustrated in Figure 3. Note that $\gamma_{L,G,1} = \{(0, s) \mid s \in (-g, g)\}$ and $\gamma_{L,G,2} = \{(s, k \frac{g}{2} \mid k = 1, 0, -1, s \in (-g, g)\}$ in this illustration. We select $\xi_L \in C_0^\infty(\mathbb{R})$ with support in $[-g + d_L^{\min}/2, g - d_L^{\min}/2]$ and the properties $0 \leq \xi_L(x) \leq 1 \ \forall x \in \mathbb{R}$, $\xi_L(x) = 1$ if

$|x| \leq g - d_L^{\min}$, and $\xi'_L(x) \leq 2(d_L^{\min})^{-1} \leq 2\mathfrak{g}d_L^{-1}$. We further select $\xi_G \in C_0^\infty(\mathbb{R}^d)$ with support in G_i^* ,

$$G_i^* = \{x \in \mathbb{R}^d \mid \exists y \in G : |x - y| < d_K, (x - y) \cdot e_i = 0\},$$

satisfying $0 \leq \xi_G(x) \leq 1$ for all $x \in \mathbb{R}^d$, $\xi_G(x) = 1$ for all $x \in G$ with $|x_i| \leq g - d_L^{\min}$, and $|\nabla \xi_G(x)| \leq (d_K^{\min})^{-1} \leq \mathfrak{g}d_K^{-1} \leq \mathfrak{g}d_L^{-1}$ for all $x \in \mathbb{R}^d$. We finally set $\xi_{L,G,i}(x) = \xi_L(x_i)\xi_G(x)$ for $x \in \mathbb{R}^d$,

$$U_{L,G,i}^* = \text{int supp } \xi_{L,G,i} \subset G_i^*, \quad \text{and} \quad U_{L,G,i} = \text{int } \{x \in G \mid \xi(x) = 1\} \subset U_{L,G,i}^*.$$

For notational convenience, we mostly write $U^* = U_{L,G,i}^*$ and $\xi = \xi_{L,G,i}$ in the sequel. Note that

$$(32) \quad |\nabla \xi| \leq |\xi_L \nabla \xi_G| + |\xi'_L \xi_G| \leq 3\mathfrak{g}d_L^{-1}.$$

Extending $v \in \mathcal{H}$ from \mathbf{Q} to \mathbb{R}^d by zero, we define

$$D_i^h v = \frac{1}{h} (v(x + e_i h) - v(x)), \quad v \in \mathcal{H},$$

with $|h| > 0$. Let $h > 0$ be sufficiently small to provide $-D_i^{-h}(\xi^2 D_i^h u_K) \in \mathcal{H}_K$. Then (13) yields

$$(33) \quad a(u_K, -D_i^{-h}(\xi^2 D_i^h u_K)) = \ell(-D_i^{-h}(\xi^2 D_i^h u_K)).$$

Exploiting

$$(34) \quad \Gamma^{(K)} \cap (he_i + U^*) \subset \Gamma^{(K)} \cap G_i^*$$

for sufficiently small $|h| > 0$, we get

$$\begin{aligned} & \int_{\mathbf{Q} \setminus \Gamma^{(K)}} \nabla u_K \cdot \nabla (-D_i^{-h}(\xi^2 D_i^h u_K)) \, dx \\ &= \int_{U^* \setminus \Gamma^{(K)}} |\nabla D_i^h u_K|^2 \xi^2 \, dx + \int_{U^* \setminus \Gamma^{(K)}} \nabla D_i^h u_K \cdot \nabla (\xi^2) D_i^h u_K \, dx. \end{aligned}$$

Similarly, (34) leads to

$$\int_{\Gamma_k} A[u_K] [-D_i^{-h}(\xi^2 D_i^h u_K)] \, d\Gamma_k = \int_{U^* \cap \Gamma_k} A[D_i^h u_K]^2 \xi^2 \, d\Gamma_k$$

for all $k = 1, \dots, K$. Utilizing (34), the fundamental theorem of calculus and a density argument, it can be shown that

$$(35) \quad \int_{U^*} |D_i^{-h} v|^2 \, dx \leq \int_{U^* \setminus \Gamma^{(K)}} |\partial_i v|^2 \, dx \quad \forall v \in \mathcal{H}.$$

Together with the Cauchy-Schwarz inequality and $U^* \subset G_i^*$ this leads to

$$\begin{aligned} |\ell(-D_i^{-h}(\xi^2 D_i^h u_K))| &\leq \|f\|_{L^2(G_i^*)} \|D_i^{-h}(\xi^2 D_i^h u_K)\|_{L^2(U^*)} \\ &\leq \|f\|_{L^2(G_i^*)} \left(\int_{U^* \setminus \Gamma^{(K)}} |\partial_i(\xi^2 D_i^h u_K)|^2 \, dx \right)^{1/2}. \end{aligned}$$

We insert the above identities and this estimate into (33) to obtain

$$\begin{aligned} & \int_{U^* \setminus \Gamma^{(K)}} |\nabla D_i^h u_K|^2 \xi^2 \, dx + \sum_{k=1}^K (1 + \mathfrak{c})^k C_k \int_{U^* \cap \Gamma_k} A[D_i^h u_K]^2 \xi^2 \, d\Gamma_k \\ &\leq \|f\|_{L^2(G_i^*)} \left(\int_{U^* \setminus \Gamma^{(K)}} |\partial_i(\xi^2 D_i^h u_K)|^2 \, dx \right)^{1/2} + \int_{U^* \setminus \Gamma^{(K)}} |\nabla D_i^h u_K| |\nabla(\xi^2)| |D_i^h u_K| \, dx. \end{aligned}$$

Now (32) and multiple applications of Young's inequality yield

$$\begin{aligned} \int_{U^* \setminus \Gamma(K)} |\nabla D_i^h u_K|^2 \xi^2 dx &\leq 2 \|f\|_{L^2(G_i^*)}^2 + 9 \mathfrak{g}^2 d_L^{-2} \|\xi D_i^h u_K\|_{L^2(G_i^*)}^2 + 36 \mathfrak{g}^2 d_L^{-2} \|D_i^h u_K\|_{L^2(G_i^*)}^2 \\ &\quad + \frac{1}{4} \int_{U^* \setminus \Gamma(K)} |\nabla D_i^h u_K|^2 \xi^4 dx + \frac{1}{4} \int_{U^* \setminus \Gamma(K)} |\nabla D_i^h u_K|^2 \xi^2 dx. \end{aligned}$$

Utilizing $\xi^4 \leq \xi^2 \leq 1$ and (35), this leads to

$$\int_{U_{L,G,i}} |\nabla D_i^h u_K|^2 dx \leq c \left(\|f\|_{L^2(G_i^*)}^2 + d_L^{-2} \|\partial_i u_K\|_{L^2(G_i^* \setminus \Gamma(K))}^2 \right).$$

Now the desired regularity $\partial_i u_K \in H^1(U_{L,G,i})$ and the corresponding a priori estimate

$$(36) \quad \|\nabla \partial_i u_K\|_{L^2(U_{L,G,i})}^2 \leq c \left(\|f\|_{L^2(G_i^*)}^2 + d_L^{-2} \|\partial_i u_K\|_{L^2(G_i^* \setminus \Gamma(K))}^2 \right)$$

are a consequence of [15, Chapter 5.8.2, Theorem 3].

It remains to show the a priori bound (31). Let $i = 1, \dots, d$ be fixed, $\gamma = \gamma_{L,G,i}$, and $G_\gamma \in \mathcal{G}^{(L)}$ such that γ is a $(d-1)$ -face of G_γ . Utilizing affine transformations of $G_\gamma \cap U_{L,G,i}$ and γ to the reference domains $(0,1)^d$ and $(0,1)^{d-1} \times \{0\}$, respectively, we obtain

$$\int_\gamma |v|^2 d\gamma \leq C \mathfrak{g}^d \left(d d_L^2 \|\nabla v\|_{L^2(G_\gamma \cap U_{L,G,i})}^2 + \|v\|_{L^2(G_\gamma \cap U_{L,G,i})}^2 \right) \quad \forall v \in H^1(G_\gamma \cap U_{L,G,i})$$

with the generic constant C emerging from the trace theorem on $(0,1)^d$. Now (31) follows by inserting $v = \partial_i u_K$ and utilizing the a priori estimate (36). \square

After these preparations, we are ready to state the main result of this section.

Theorem 4.2. *For each $K \in \mathbb{N}$, the approximate solution u_K of Problem 2.3 satisfies the error estimate*

$$(37) \quad \|u - u_K\|^2 \leq C \left(\sup_{k>K} C_k^{-1} d_k^{-1} \right) \|f\|_{L^2(Q)}^2 (1 + \mathfrak{c})^{-K}$$

with C only depending on the space dimension d , shape regularity \mathfrak{g} in (30), coercivity \mathfrak{a} in (11), the Poincaré-type constant C_0 in (19) and on the material constant \mathfrak{c} in (7).

Proof. For $u \neq u_K$ we get the residual error estimate

$$\|u - u_K\| \leq \mathfrak{a}^{-1} r_K(u - u_K) / \|u - u_K\| \leq \mathfrak{a}^{-1} \|r_K\|_{\mathcal{H}'},$$

which trivially holds for $u = u_K$ as well. Hence, we derive an upper bound for $\|r_K\|_{\mathcal{H}'}$.

Let $G \in \mathcal{G}^{(K)}$ and $\tilde{G} \in \mathcal{G}^{(L)}$ for some $L > K$ such that $\tilde{G} \subset G$. Furthermore, let ν and $\tilde{\nu}$ be the outer normal of G and \tilde{G} respectively. We first observe that $-\Delta u_K = f$ on G with $-\partial_\nu u_K = \llbracket u_K \rrbracket$ on ∂G . In particular, we note that $\nabla u_K \cdot \nu \in L^2(\partial G)$. Furthermore, by the regularity obtained in Lemma 4.1, we see that $\nabla u_K \cdot \tilde{\nu} \in L^2(\partial \tilde{G})$. Now we can use a version of Green's formula proved by Casas and Fernández [9, Corollary 1], exploiting (in the notation of [9]) that $\nabla u_K \in W^2(\text{div}, G)$ and $v \in W^1(\tilde{G}) \cap L^\infty(\tilde{G})$, to obtain

$$(38) \quad r_K(v) = \ell(v) - a(u_K, v) = \sum_{k=K+1}^L \int_{\Gamma_k} \partial_\nu u_K \llbracket v \rrbracket d\Gamma_k$$

for any test function $v \in \mathcal{C}_{L,0}^1(\mathbf{Q})$. The Cauchy-Schwarz inequality then yields

$$\begin{aligned} r_K(v) &= \sum_{k=K+1}^L \int_{\Gamma_k} \left((1+\mathfrak{c})^{-k/2} C_k^{-1/2} \partial_\nu u_K \right) \left((1+\mathfrak{c})^{k/2} C_k^{1/2} \llbracket v \rrbracket \right) d\Gamma_k \\ &\leq \left(\sum_{k=K+1}^L \int_{\Gamma_k} (1+\mathfrak{c})^{-k} C_k^{-1} |\partial_\nu u_K|^2 d\Gamma_k \right)^{1/2} \|v\|. \end{aligned}$$

Since L can be arbitrarily large, we infer

$$\|r_K\|_{\mathcal{H}'}^2 \leq \left(\sup_{k>K} C_k^{-1} d_k^{-1} \right) \left(\sup_{k>K} d_k \|\partial_\nu u_K\|_{L^2(\Gamma_k)}^2 \right) (1+\mathfrak{c})^{-K} \left(\sum_{k=1}^{\infty} (1+\mathfrak{c})^{-k} \right)$$

and Lemma 4.1 provides the a priori estimate

$$\begin{aligned} d_k \|\partial_\nu u_K\|_{L^2(\Gamma_k)}^2 &= \sum_{G \in \mathcal{G}^{(K)} \setminus \mathcal{G}_\infty^{(K)}} \sum_{i=1}^d d_k \|\partial_i u_K\|_{L^2(\gamma_{k,D,i})}^2 \\ &\leq 3dc \left(d_k^2 \|f\|_{L^2(\mathbf{Q})}^2 + \|\nabla u_K\|_{L^2(\mathbf{Q} \setminus \Gamma^{(K)})}^2 \right) \leq C \|f\|_{L^2(\mathbf{Q})}^2 \end{aligned}$$

for all $k > K$ with C depending only on $d, \mathbf{g}, \mathbf{a}$, and the Poincaré-type constant C_0 in (19). This concludes the proof. \square

Recall that the factor $\sup_{k>K} C_k^{-1} d_k^{-1}$ depends on the geometry of the actual interface network.

Remark 4.3. For the Cantor interface network described in Example 2.1, we have $C_K^{-1} d_K^{-1} = 2$ for all $K \in \mathbb{N}$. Hence, Theorem 4.2 implies exponential convergence of the solution u_K of the level- K interface Problem 2.3 to the solution u of the fractal interface Problem 3.11 according to the error estimate

$$\|u - u_K\| \leq C \|f\|_{L^2(\mathbf{Q})} (1+\mathfrak{c})^{-K}$$

with C only depending on $d, \mathbf{g}, \mathbf{a}, \mathfrak{c}$, and on the Poincaré-type constant C_0 in (19).

Remark 4.4. The exponential decay of $\|u - u_K\|$ is essentially due to the exponential growth of the weights $(1+\mathfrak{c})^k$ on the interfaces. It is an interesting question for future investigations whether these weights can be replaced by another monotonically increasing function $f(k)$. However, note that the Poincaré-type inequality (19) indicates exponential growth of $f(k)$.

5. NUMERICAL COMPUTATIONS

Let $\mathcal{T}^{(1)}$ be a partition of \mathbf{Q} into simplices with maximal diameter $h_1 > 0$ which is regular in the sense that the intersection of two simplices from $\mathcal{T}^{(1)}$ is either a common n -simplex for some $n = 0, \dots, d$ or empty. Then $\mathcal{T}^{(K)}$ denotes the partition of \mathbf{Q} resulting from $K-1$ uniform regular refinements of $\mathcal{T}^{(1)}$ (cf., e.g., [6, 8]) for each $K \in \mathbb{N}$. The maximal diameter is $h_K = h_1 2^{K-1}$, and $\mathcal{N}^{(K)}$ stands for the set of vertices of simplices in $\mathcal{T}^{(K)}$. We assume that the partition $\mathcal{T}^{(K)}$ resolves the piecewise affine interface network $\Gamma^{(K)}$, i.e., for all $k \leq K$ the interfaces Γ_k can be represented as a sequence of $(d-1)$ -faces of simplices from $\mathcal{T}^{(K)}$. For each $K \in \mathbb{N}$ and each $G \in \mathcal{G}^{(K)}$, we introduce the space $\mathcal{S}_G^{(K)}$ of piecewise affine finite elements with

respect to the local partition $\mathcal{T}_G^{(K)} = \{T \in \mathcal{T}^{(K)} \mid T \subset \overline{G}\}$. The discretization of the level- K interface Problem 2.3 with respect to the corresponding broken finite element space

$$\mathcal{S}^{(K)} = \{v : \mathbf{Q} \rightarrow \mathbb{R} \mid v|_G \in S_G^{(K)} \forall G \in \mathcal{G}^{(K)}\} \subset \mathcal{H}_K$$

amounts to finding $\tilde{u}_K \in \mathcal{S}^{(K)}$ such that

$$(39) \quad a(\tilde{u}_K, v) = \ell(v) \quad \forall v \in \mathcal{S}^{(K)}.$$

For each $K \in \mathbb{N}$, existence and uniqueness of a solution follows from the Lax-Milgram lemma.

5.1. Exponential convergence of multiscale interface problems. In case of the Cantor interface network (cf. Example 2.1) the solutions u_K of the level- K interface Problem 2.3 for $K \in \mathbb{N}$ converge exponentially to the solution u of the fractal interface Problem 3.11 (cf. Remark 4.3). For a numerical illustration, we consider this example in $d = 2$ space dimensions with $\mathfrak{c} = 1$, $f \equiv 1$, $A \equiv 1$, and the geometrical parameter $C_K = 2^{K-1}$. Note that the $\|\cdot\|$ norm in \mathcal{H} (cf. (25)) is identical with the energy norm induced by $a(\cdot, \cdot)$ (cf. (27)) in this instance.

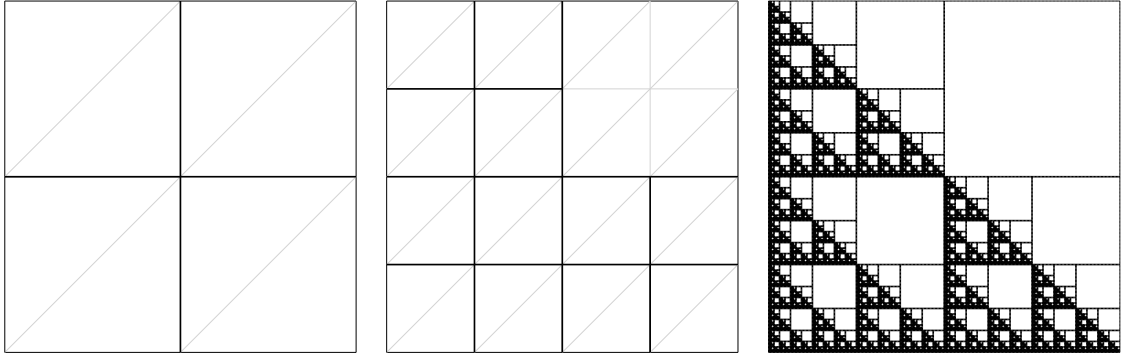


FIGURE 4. Initial triangulation $\mathcal{T}^{(1)}$, uniform refinement $\mathcal{T}^{(2)}$ together with the Cantor interface network $\Gamma^{(K)}$ for $K = 1, 2$, and 8 in $d = 2$ space dimensions

The initial triangulation $\mathcal{T}^{(1)}$ with $h_1 = 2^{-1}$ is depicted in the left picture of Figure 4 (grey) together with the initial Cantor network $\Gamma^{(1)}$ (black). Successive uniform refinement of $\mathcal{T}^{(1)}$ provides the triangulations $\mathcal{T}^{(K)}$ with $h_K = 2^{-K}$ resolving the interfaces $\Gamma^{(K)}$ on subsequent levels K . The case $K = 2$ is illustrated in the middle while the right picture of Figure 4 shows the Cantor network $\Gamma^{(8)}$.

The linear systems associated with the corresponding finite element discretizations (39) on each level K are solved directly. Exploiting

$$\|u - u_K\| \leq \|u - u_9\| + \|u_9 - u_K\|, \quad K \in \mathbb{N},$$

the fractal homogenization error is replaced by the heuristic error estimate

$$(40) \quad e_K = \|\tilde{u}_{10} - \tilde{u}_9\| + \|\tilde{u}_9 - \tilde{u}_K\|, \quad K = 1, \dots, 8.$$

The first term in (40) is intended to capture the error made by resolving a “large” but finite number of interfaces instead of infinitely many, while the second term aims at the additional contribution made by resolving only the actual “small” number of $K = 1, \dots, 8$ levels.

Figure 5 shows the error estimates e_K over the levels K (dotted line) together with the expected asymptotic bound of order $(1 + \mathfrak{c})^{-K}$ (solid line) for $K = 1, \dots, 8$. Both curves have

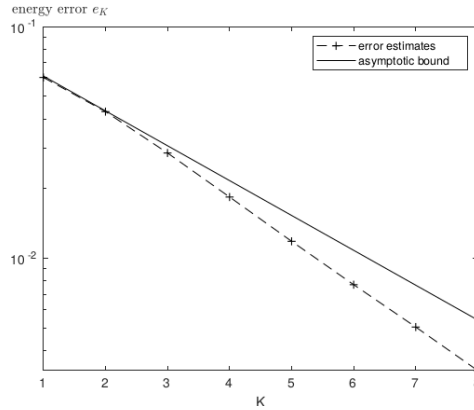


FIGURE 5. Exponential decay of fractal homogenization error

very similar slope which nicely confirms our theoretical findings. As $\|u - u_9\| \geq \|u_{10} - u_9\|$ and $\|\tilde{u}_9 - \tilde{u}_K\| = 0$ for $K = 9$, we would expect that e_K underestimates the fractal homogenization error for increasing K . This could explain the slight deviation from the expected asymptotic behavior.

5.2. Fractal numerical homogenization. Aiming at an iterative solution of the discrete problems (39) with a convergence speed that is independent of the number of levels $K \in \mathbb{N}$, we now present a multilevel preconditioner in the spirit of [26, 27].

To this end, we introduce the sets of local patches

$$Q^{(k)} = \begin{cases} \{\overline{Q}\} & \text{for } k = 1 \\ \{\omega_x^{(k)} \subset \overline{Q} \mid x \in \mathcal{N}^{(k-1)}\} & \text{for } k \geq 2 \end{cases}$$

with $\omega_x^{(k)} \subset \overline{Q}$ consisting of all simplices $T \in \mathcal{T}^{(k-1)}$ with common vertex $x \in \mathcal{N}^{(k-1)}$. The decomposition of Q into patches $\omega \in Q^{(k)}$ gives rise to the decomposition

$$(41) \quad S^{(k)} = \sum_{\omega \in Q^{(k)}} S_{\omega}^{(k)}, \quad k \in \mathbb{N},$$

into the local finite element spaces

$$S_{\omega}^{(k)} = \{v \in S^{(k)} \mid v|_{Q \setminus \text{int } \omega} = 0\}, \quad \omega \in Q^{(k)}.$$

For each fixed $K \in \mathbb{N}$, this leads to the splitting

$$S^{(K)} = \sum_{k=1}^K \sum_{\omega \in Q^{(k)}} S_{\omega}^{(k)}$$

and the corresponding multilevel preconditioner [35, 36]

$$(42) \quad T_K = \sum_{k=0}^K \sum_{\omega \in Q^{(k)}} P_{S_{\omega}^{(k)}}.$$

with $P_V : S^{(K)} \rightarrow V$ denoting the Ritz projection,

defined by

$$(43) \quad a(P_V w, v) = a(w, v), \quad \forall v \in V.$$

Note that the evaluation of each local projection $P_{S_{\omega}^{(k)}}$ amounts to the solution of a (small) self-adjoint linear system on the patch $\omega \in \mathcal{Q}^{(k)}$. Therefore, T_K can be regarded as a multilevel version of the classical block Jacobi preconditioner.

The analysis of upper bounds for the condition number of T_K as well as fractal counterparts of multiscale finite elements [25, 28] will be considered in a separate publication.

5.2.1. Cantor interface network. We consider the level- K interface Problem 2.3 for the Cantor interface network with parameters, finite element discretization, and initial triangulation $\mathcal{T}^{(1)}$ as previously described in subsection 5.1.

Let $\tilde{u}_K^{(\nu)}$, $\nu \in \mathbb{N}$, denote the iterates of the preconditioned conjugate gradient method with preconditioner T_K given in (42) and initial iterate $\tilde{u}_K^{(0)} = \tilde{u}_0$. The corresponding algebraic error reduction factors

$$(44) \quad \rho_K^{(\nu)} = \frac{\|\tilde{u}_K - \tilde{u}_K^{(\nu)}\|}{\|\tilde{u}_K - \tilde{u}_K^{(\nu-1)}\|}$$

of each iteration step are depicted in Figure 6 for $\nu = 1, \dots, 8$ together with their geometric average ρ_K for $K = 5, \dots, 9$. The averaged reduction factors ρ_K seem to saturate with increasing level K .

ν	$K = 5$	$K = 6$	$K = 7$	$K = 8$	$K = 9$
1	0.479	0.481	0.481	0.482	0.482
2	0.445	0.464	0.483	0.500	0.514
3	0.453	0.448	0.442	0.437	0.439
4	0.429	0.452	0.474	0.493	0.503
5	0.451	0.465	0.468	0.472	0.477
6	0.432	0.444	0.459	0.477	0.494
7	0.447	0.467	0.463	0.456	0.455
8	0.450	0.483	0.487	0.489	0.490
ρ_K	0.448	0.463	0.469	0.475	0.481

FIGURE 6. Algebraic error reduction factors for the Cantor interface network

In practical computations, it is sufficient to reduce the algebraic error $\|\tilde{u}_K - \tilde{u}_K^{(\nu)}\|$ up to discretization accuracy $\|u_K - \tilde{u}_K\|$. Galerkin orthogonality implies

$$\|\tilde{u}_{K+1} - \tilde{u}_K\|^2 + \|u - \tilde{u}_{K+1}\|^2 = \|u - \tilde{u}_K\|^2.$$

We utilize the stopping criterion

$$(45) \quad \|\tilde{u}_K - \tilde{u}_K^{(\nu_0)}\| \leq \|\tilde{u}_{K+1} - \tilde{u}_K\| \leq \|u - \tilde{u}_K\|$$

provided by the resulting lower bound for the discretization error and the final iterate on the preceding level $K - 1$ as the initial iterate on the actual level K (nested iteration). Then, only $\nu_0 = 1$ step of the preconditioned conjugate gradient iteration is sufficient to provide an approximation $\tilde{u}_K^{(\nu_0)}$ of \tilde{u}_K with discretization accuracy for all $K = 2, \dots, 9$.

5.2.2. *Layered interfaces.* We consider the level- K interface Problem 2.3 in $d = 2$ space dimensions with parameters $\mathfrak{c} = 1$, $f \equiv 1$, $A \equiv 1$, and non-intersecting interfaces $\Gamma_k \subset \mathbf{Q} = (0, 1)^2$ described as follows. Figure 7 shows the initial triangulation $\mathcal{T}^{(1)}$ (grey) with $h_1 = 2^{-4}$ together with the 3 macro interfaces forming $\Gamma^{(1)}$. Again, $\mathcal{T}^{(k)}$ is obtained by uniform refinement of $\mathcal{T}^{(1)}$ and $\Gamma_k = \Gamma^{(K)} \setminus \Gamma^{(K-1)}$ is composed of 6 randomly selected, non-intersecting polygons consisting of edges of triangles $T \in \mathcal{T}^{(K)}$ one above and one below each macro interface from $\Gamma^{(1)}$. For $K = 2$, this is illustrated in the middle picture of Figure 7. Note that at most $C_K = 2^K - 1$ interfaces are cut by any straight line through \mathbf{Q} . The final interface $\Gamma^{(6)}$ is displayed in the right picture.

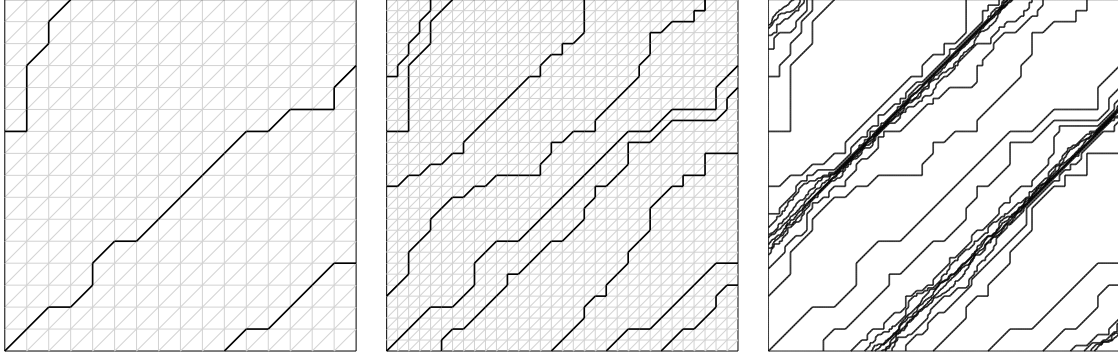


FIGURE 7. Initial triangulation $\mathcal{T}^{(1)}$, uniform refinement $\mathcal{T}^{(2)}$ together with the layered interface network $\Gamma^{(K)}$ for $K = 1, 2$, and 6

ν	$K = 2$	$K = 3$	$K = 4$	$K = 5$	$K = 6$
1	0.303	0.377	0.376	0.392	0.423
2	0.177	0.431	0.473	0.496	0.523
3	0.329	0.316	0.418	0.492	0.542
4	0.372	0.404	0.405	0.497	0.517
5	0.247	0.409	0.501	0.503	0.525
6	0.329	0.405	0.421	0.497	0.533
7	0.366	0.362	0.458	0.488	0.539
8	0.328	0.440	0.426	0.497	0.527
ρ_K	0.299	0.391	0.433	0.481	0.515

FIGURE 8. Algebraic error reduction factors for the layered interface network

As in Subsection 5.2.1, we consider the conjugate gradient iteration with the multilevel preconditioner defined in (42) and initial iterate $u_K^{(0)} = \tilde{u}_0$ for $K = 2, \dots, 6$. Figure 8 shows the algebraic error reduction factors $\rho_K^{(\nu)}$ defined in (44), together with their geometric average ρ_K . The averaged reduction factors ρ_K are slightly increasing with increasing level K .

If nested iteration is applied, only one iteration step is needed to reach discretization accuracy according to the stopping criterion (45) in Subsection 5.2.1.

REFERENCES

- [1] Grégoire Allaire. Homogenization and two-scale convergence. *SIAM Journal on Mathematical Analysis*, 23(6):1482–1518, 1992.
- [2] Grégoire Allaire and Marc Briane. Multiscale convergence and reiterated homogenisation. *Proceedings of the Royal Society of Edinburgh Section A: Mathematics*, 126(2):297–342, 1996.
- [3] Scott Armstrong, Tuomo Kuusi, and Jean-Christophe Mourrat. Quantitative stochastic homogenization and large-scale regularity. *arXiv preprint arXiv:1705.05300*, 2017.
- [4] Scott N. Armstrong and Charles K. Smart. Quantitative stochastic homogenization of elliptic equations in nondivergence form. *Archive for Rational Mechanics and Analysis*, 214(3):867–911, 2014.
- [5] Leonardo Baffico, Céline Grandmont, Yvon Maday, and Axel Osses. Homogenization of elastic media with gaseous inclusions. *Multiscale Modeling & Simulation*, 7(1):432–465, 2008.
- [6] Randolph E. Bank, Andrew H. Sherman, and Alan Weiser. Some refinement algorithms and data structures for regular local mesh refinement. *Scientific Computing, Applications of Mathematics and Computing to the Physical Sciences*, 1:3–17, 1983.
- [7] Yehuda Ben-Zion and Charles G. Sammis. Characterization of fault zones. *Pure and Applied Geophysics*, 160(3-4):677–715, 2003.
- [8] Jürgen Bey. Simplicial grid refinement: on Freudenthal’s algorithm and the optimal number of congruence classes. *Numerische Mathematik*, 85(1):1–29, 2000.
- [9] Eduardo Casas and Luis Alberto Fernández. A green’s formula for quasilinear elliptic operators. *Journal of mathematical analysis and applications*, 142(1):62–73, 1989.
- [10] Paul Cazeaux, Céline Grandmont, and Yvon Maday. Homogenization of a model for the propagation of sound in the lungs. *Multiscale Modeling & Simulation*, 13(1):43–71, 2015.
- [11] Doina Cioranescu, Alain Damlamian, Patrizia Donato, Georges Griso, and Rachad Zaki. The periodic unfolding method in domains with holes. *SIAM Journal on Mathematical Analysis*, 44(2):718–760, 2012.
- [12] Doina Cioranescu, Alain Damlamian, and Julia Orlik. Homogenization via unfolding in periodic elasticity with contact on closed and open cracks. *Asymptotic Analysis*, 82(3-4):201–232, 2013.
- [13] Patrizia Donato and Sara Monsurro. Homogenization of two heat conductors with an interfacial contact resistance. *Analysis and Applications*, 2(03):247–273, 2004.
- [14] Yalchin Efendiev and Thomas Y. Hou. *Multiscale Finite Element Methods: Theory and Applications*, volume 4. Springer Science & Business Media, 2009.
- [15] Lawrence C. Evans. *Partial Differential Equations*. American Mathematical Society, 1998.
- [16] Xiang Gao and Kelin Wang. Strength of stick-slip and creeping subduction megathrusts from heat flow observations. *Science*, 345(6200):1038–1041, 2014.
- [17] Antoine Gloria, Stefan Neukamm, and Felix Otto. An optimal quantitative two-scale expansion in stochastic homogenization of discrete elliptic equations. *ESAIM: Mathematical Modelling and Numerical Analysis*, 48(2):325–346, 2014.
- [18] Georges Griso. Error estimate and unfolding for periodic homogenization. *Asymptotic Analysis*, 40(3, 4):269–286, 2004.
- [19] Isabelle Gruais and Dan Poliřevski. Heat transfer models for two-component media with interfacial jump. *Applicable Analysis*, 96(2):247–260, 2017.
- [20] Martin Heida. An extension of the stochastic two-scale convergence method and application. *Asymptotic Analysis*, 72(1-2):1–30, 2011.
- [21] Martin Heida. Stochastic homogenization of heat transfer in polycrystals with nonlinear contact conductivities. *Applicable Analysis*, 91(7):1243–1264, 2012.
- [22] Ulrich Hornung. *Homogenization and Porous Media*, volume 6. Springer Science & Business Media, 2012.
- [23] Hans-Karl Hummel. *Homogenization of Periodic and Random Multidimensional Microstructures*. PhD thesis, Technische Universität Bergakademie Freiberg, 1999.
- [24] Vasilii Vasil’evich Jikov, Sergei M. Kozlov, and Olga Arsen’evna Oleřnik. *Homogenization of Differential Operators and Integral Functionals*. Springer-Verlag, Berlin, 1994.
- [25] Ralf Kornhuber, Daniel Peterseim, and Harry Yserentant. An analysis of a class of variational multiscale methods based on subspace decomposition. *Mathematics of Computation*, 87(314):2765–2774, 2018.
- [26] Ralf Kornhuber, Joscha Podlesny, and Harry Yserentant. Direct and iterative methods for numerical homogenization. In Chang-Ock Lee, Xiao-Chuan Cai, David E. Keyes, Hyea Hyun Kim, Axel Klawonn,

- Eun-Jae Park, and Olof B. Widlund, editors, *Domain Decomposition Methods in Science and Engineering XXIII*, pages 217–225. Springer International Publishing, 2017.
- [27] Ralf Kornhuber and Harry Yserentant. Numerical homogenization of elliptic multiscale problems by subspace decomposition. *Multiscale Modeling and Simulation*, 14(3):1017–1036, 2016.
- [28] Axel Målqvist and Daniel Peterseim. Localization of elliptic multiscale problems. *Mathematics of Computation*, 83(290):2583–2603, 2014.
- [29] Umberto Mosco and Maria Agostina Vivaldi. Thin fractal fibers. *Mathematical Methods in the Applied Sciences*, 36(15):2048–2068, 2013.
- [30] Hiroyuki Nagahama and Kyoko Yoshii. Scaling laws of fragmentation. In *Fractals and Dynamic Systems in Geoscience*, pages 25–36. Springer, 1994.
- [31] Onno Oncken, David Boutelier, Georg Dresen, and Kerstin Schemmann. Strain accumulation controls failure of a plate boundary zone: Linking deformation of the central andes and lithosphere mechanics. *Geochemistry, Geophysics, Geosystems*, 13(12), 2012.
- [32] Alfio Quarteroni and Alberto Valli. *Domain decomposition methods for partial differential equations*. Oxford University Press, 1999.
- [33] Charles G. Sammis, Robert H. Osborne, J. Lawford Anderson, Mavonwe Banerdt, and Patricia White. Self-similar cataclasis in the formation of fault gouge. *Pure and Applied Geophysics*, 124(1):53–78, 1986.
- [34] Donald L. Turcotte. Crustal deformation and fractals, a review. In Jörn H. Kruhl, editor, *Fractals and Dynamic Systems in Geoscience*, pages 7–23. Springer, 1994.
- [35] Jinchao Xu. Iterative methods by space decomposition and subspace correction. *SIAM Review*, 34(4):581–613, 1992.
- [36] Harry Yserentant. Old and new convergence proofs for multigrid methods. *Acta Numerica*, 2:285–326, 1993.
- [37] Vasili Vasil’evich Zhikov and Aleksandr L. Pyatnitskiĭ. Homogenization of random singular structures and random measures. *Izvestiya Rossiiskaya Akademiya Nauk. Seriya Matematicheskaya*, 70(1):23–74, 2006.